J Mater Sci (2011) 46:3812–3821
DOI 10.1007/s10853-011-5295-0

Investigation of active slip-systems in some body-centered cubic metals

Dilawar Ali · Nasreen Mushtaq · M. Z. Butt

Received: 28 July 2010 / Accepted: 17 January 2011 / Published online: 8 February 2011

Abstract Tensile tests were performed on high-purity W and Mo polycrystals at room temperature for a range of axial strain-rates 2.1×10^{-4}–2.1×10^{-2} s^{-1}. The critical resolved shear stress (CRSS) data was analyzed by using the analytical formulation for the strain-rate dependence of the CRSS derived in the kink-pair nucleation (KPN) model of flow stress in crystals with high intrinsic lattice friction. On evaluation of various microscopic slip-parameters of the model, the active slip-system in both W and Mo polycrystals was identified as $\{110\}\langle 111\rangle$. This is in good agreement with that deduced from the published data on the temperature dependence of the CRSS of these crystals as well as from the observed slip-lines on the deformed crystals reported in the literature. Moreover, the available data on the temperature dependence of the CRSS of Mo, Nb, Fe, V, and K crystals were also analyzed within the framework of the KPN model of flow stress. Peierls mechanism was found to be responsible for the CRSS of these metals; the active slip-systems in refractory metals Mo, Nb, Fe, and V were $\{110\}\langle 111\rangle$ and $\{211\}\langle 111\rangle$ whereas that in alkali metal K was $\{321\}\langle 111\rangle$.

Introduction

Deformation behavior of crystalline materials has been under investigation since the idea of linear defects or dislocations in crystals was conceived by Orowan [1], Polanyi [2], and Taylor [3, 4] independently. The observed initial flow stress or yield stress of real crystals, which is far less than the theoretically predicted one for ideal crystals, was attributed to the ease with which dislocations can glide in certain crystallographic planes under the action of applied force. Experiments show that the yield stress of crystals is dependent on the imposed deformation-rate as well as on the temperature at which deformation is carried out, in addition to the orientation of single crystals and the grain size of polycrystals. As far as the slip system responsible for the deformation of single crystals is concerned, slip is likely to occur on a slip-system when the resolved shear stress exceeds a critical value given by Schmid law. In face-centered cubic (fcc) single crystals, there are twelve such possible slip-systems, namely $\{111\}\langle 110\rangle$ [5] but the assortment of active slip-systems in body-centered cubic (bcc) single crystals has been a long-standing problem in crystal plasticity theory.

Investigations of the active slip-systems involved in the deformation of bcc metals have been carried out extensively through slip-line observations over the past four decades (e.g., [6–11]). As a result of extensive experimentation, there is consensus on the most densely packed $\langle 111\rangle$ directions as the slip directions whereas the observed slip planes are the crystallographic planes $\{110\}$, $\{211\}$, and $\{321\}$, which belong to the $\langle 111\rangle$ zone. The type and number of the active slip-planes depend on the crystallographic orientation of the stress axis, purity of the crystal as well as on the deformation parameters, like temperature and imposed strain-rate.

Kaun et al. [6] investigated the slip line patterns and the active slip-systems of zone-refined W and Mo single crystals for a range of crystallographic orientations of the crystal axis. They deformed cylinder-shaped tensile specimens of these metals in tension at a strain-rate $<10^{-4}$ s^{-1} at room temperature, and used optical as well as electron microscope to study the slip lines. They found that slip

D. Ali (✉) · N. Mushtaq · M. Z. Butt
Department of Physics, University of Engineering and Technology, G. T. Road, Lahore 54890, Pakistan
e-mail: dilawarphysics@gmail.com

occurred preferentially on the {110} planes, but further slip planes of the ⟨111⟩ zone were also active to some extent. A valid theory of flow stress in crystals with high intrinsic lattice friction must therefore be able to account for the observations referred to above.

The main objective of this study was to perform deformation tests on high-purity W and Mo polycrystals at room temperature for a range of tensile strain-rates, and to analyze the data within the framework of the kink-pair nucleation (KPN) model of flow stress [12, 13], in which analytical formulation of the strain-rate dependence of the critical resolved shear stress (CRSS) at a given temperature facilitates the determination of the slip system responsible for plastic deformation. The observed temperature dependence of the CRSS of Mo polycrystals deformed by Galygin [14] at a given tensile strain-rate $\sim 10^{-4}\ s^{-1}$ between 200 and 330 K will also be analyzed with the help of the KPN model formulation for the temperature dependence of the CRSS at a given strain-rate, and the slip system identified so will be compared with that found via strain-rate dependence of the CRSS of Mo polycrystals in this deformation tests.

Another objective was to analyze the CRSS-T data available in the literature for a number of refractory and alkali bcc metals within the framework of the KPN model of flow stress cited above to identify the deformation mechanisms responsible for the yielding of both types of bcc metals, and examine its authenticity in the light of the slip-line observations made on the deformed crystals of these metals.

Materials and deformation tests

Wires of 99.99 wt% tungsten polycrystal were obtained from Johnson and Mathey Chemical Limited London. The main metallic impurities (in wt.ppm) were Mo(32), Ni(28), Cr(18), Al(13), and Pb(9). Specimens, 80 mm long and 2 mm in diameter, were cut from the as-received wires, and then sealed in Pyrex glass tube evacuated to 1.3 mPa (10^{-5} Torr). These were annealed for 2 h in a muffle furnace maintained at 700 °C to reduce internal stresses. The tube was allowed to cool at room temperature before taking out the specimens. Using the linear-intercept technique, the mean grain-diameter of the annealed specimens was found to be 20 μm.

The 99.972 wt% molybdenum polycrystals used were in the form of rolled sheet of 0.13 mm thickness. The main metallic impurities (in wt ppm) were Fe(200), Mn(30), Ni(30), and Cr(20). Specimens, 80 mm long and 10 mm wide, were cut from the as-received sheet, and were sealed in a Pyrex glass tube evacuated to 1.3 mPa (10^{-5} Torr). These were then annealed at 700 °C for 2 h. The tube was allowed to cool at room temperature before taking out the specimens. Using the linear-intercept technique, the mean grain-diameter of the annealed specimens was found to be 37 μm.

The annealed specimens were then deformed in tension at room temperature in a Universal Materials Testing Machine (Model 1195, Instron Ltd., UK). Tensile strain-rates used were in the range 2.1×10^{-4}–$2.1 \times 10^{-2}\ s^{-1}$ corresponding to cross-head speeds 0.5–50 mm/min. The chart of load-time recorder was driven at speeds so as to keep the chart speed to cross-head speed ratio constant. The full scale load ranges used were 2 and 5 kN. The 0.2% proof stress data corresponding to various strain-rates have been given in Table 1. Each value denotes an average of four independent measurements. The specimens deformed at the highest tensile strain-rate $2.1 \times 10^{-2}\ s^{-1}$ corresponding to 50 mm/min cross-head speed fractured without undergoing plastic deformation, and were therefore ignored. The data given in Table 1, together with that on the temperature dependence of the CRSS of some bcc metals available in the literature, will be analyzed within the framework of the KPN model [12, 13] of flow stress in crystals with high intrinsic lattice friction.

Table 1 Values of 0.2% proof stress of W and Mo polycrystals corresponding to different strain-rates

Metal	Cross head speed (mm/min)	$\dot{\varepsilon}(s^{-1})$	$\sigma_{0.2}$ (MPa)	$\sigma_{0.2}^{1/2}$ (MPa$^{1/2}$)	$\dot{\gamma}(s^{-1})$	$\tau_{0.2}$ (MPa)	$\tau_{0.2}^{1/2}$ (MPa$^{1/2}$)
W (▲)	0.5	2.1×10^{-4}	539	23.22	6.30×10^{-4}	180	13.40
	1.0	4.2×10^{-4}	563	23.73	1.26×10^{-3}	188	13.70
	2.0	8.4×10^{-4}	584	24.17	2.52×10^{-3}	195	13.95
	5.0	2.1×10^{-3}	618	24.86	6.30×10^{-3}	206	14.35
	10	4.2×10^{-3}	648	25.46	1.26×10^{-2}	216	14.70
Mo (■)	0.5	2.1×10^{-4}	423	20.57	6.30×10^{-4}	141	11.87
	1.0	4.2×10^{-4}	450	21.21	1.26×10^{-3}	150	12.25
	2.0	8.4×10^{-4}	506	22.49	2.52×10^{-3}	169	12.99
	5.0	2.1×10^{-3}	577	24.02	6.30×10^{-3}	192	13.87
	10	4.2×10^{-3}	608	24.66	1.26×10^{-2}	203	14.24

Theoretical considerations

In the KPN model of flow stress in crystals with high intrinsic lattice friction [12], the unit activation process of yielding comprises stress-assisted, thermally activated, nucleation of a kink-pair in the $(a_0/2)\langle 111\rangle$ screw dislocation trapped in a Peierls valley, leading to its forward movement over the Peierls hill to the next Peierls valley, after attainment of the saddle-point configuration. At temperatures below 0.1–0.2 T_{melt}, where diffusional processes are dormant in the crystal, the activation energy (free enthalpy), $W(\tau)$, for the formation of a kink-pair of critical maximum height, nb, for saddle-point configuration is given by [12]:

$$W = 2W_0 - 2\alpha_0\tau^{1/2}, \tag{1}$$

with the yield criterion

$$W = mkT, \tag{2}$$

where

$$m = \ln(\dot{\gamma}_0/\dot{\gamma}) = 25 \pm 2.3. \tag{3}$$

Here $W_0 = n(UGb^3)^{1/2}$, $\alpha_0 = (1/2)(nb)^{3/2}\,(Gb^3)^{1/2}$, G is the shear modulus, U is the Peierls energy per interatomic spacing along the screw dislocation, $2W_0$ is the kink-pair formation energy W_{kp} at $\tau = 0$, k is the Boltzmann constant, $\dot{\gamma}$ is the shear rate of the crystal with typical values in the range 10^{-3}–10^{-5} s^{-1}, and the pre-exponential factor $\dot{\gamma}_0$ is of the order of 10^7 s^{-1}.

Since the discrete atomic processes involved in the passage of a dislocation over the Peierls barrier are not known exactly, therefore precise calculation of the critical maximum height, nb, of the kink-pair for saddle-point configuration (n is a numerical constant and b is the length of the Burgers vector) is rather difficult. However, one can visualize that nb can be at the most equal to the distance a between two consecutive Peierls valleys (Fig. 1), as the formation of the kinks having a height larger than the inter-valley distance is hardly probable. Thus, for two consecutive Peierls valleys along $\langle 111\rangle$ direction in bcc crystals, one finds that when $nb = a$, the value of $n = (a/b)$ will be 0.9428, 1.6329, and 2.4945 for {110}, {211}, and {321} slip planes, respectively. On the other hand, the screw-dislocation segment escaped from the Peierls valley PV_1 will not be able to cross the Peierls hill PH if maximum height, nb, of the kink-pair is less than $a/2$, i.e., $n < (a/2b)$, and hence slip will not occur. At the CRSS, one would therefore expect the critical maximum activation distance nb for saddle-point configuration to lie in the range $(a/2) < nb \leq a$. In case nb is less than a but greater than $a/2$, further "unpinning" at the corners of the bulge, accompanied by "repinning" at the leading edge, completes the advance of the dislocation segment to the next Peierls valley PV_2. According to Feltham and Kauser [15], the unpinning at the corners of the bulge, in the post-nucleation growth stage of the area of slip, would require an activation energy low compared with that for saddle-point configuration, and would not be rate determining in the glide process.

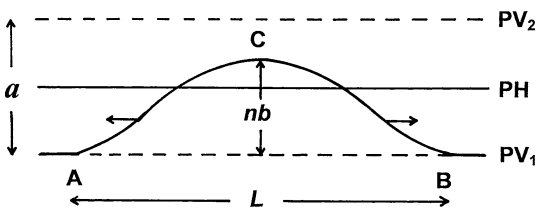

Fig. 1 Transition of a screw dislocation segment between two consecutive Peierls valleys PV_1 and PV_2 over the Peierls hill PH [12]

One can also re-write Eq. 1 in terms of deformation temperature T as follows:

$$\tau^{1/2} = A - BT, \tag{4}$$

where

$$A = (W_0/\alpha_0) = \tau_0^{1/2},\ B = (mk/2\alpha_0) \text{ and } \tau_0 = \left(4U/nb^3\right).$$

Equation 4 shows that for a given strain-rate (i.e., if m is constant), $\tau^{1/2}$ of crystals with high intrinsic lattice friction decreases linearly with the increase in temperature T. The value of A is in fact the intercept made on the stress axis at $T \to 0$ K on extrapolation of the $\tau^{1/2}$–T straight line fitted to the data, and helps to determine τ_o, i.e., the CRSS at $T \to 0$ K. Similarly B, the magnitude of the slope of the $\tau^{1/2}$–T line, helps to evaluate the parameter α_0, and this together with A then yields the value of W_0, i.e., formation energy of a solitary kink. Moreover, the intercept made by the $\tau^{1/2}$–T line on the temperature axis for $\tau = 0$ provides the so-called knee temperature $T_k = (A/B) = (2W_0/mk)$, which also facilitates the determination of W_0.

As far as the dependence of the CRSS τ on the shear rate $\dot{\gamma}$ at a constant temperature T is concerned, Butt et al. [13], on re-writing Eq. 4 in conjunction with Eqs. 2–3, derived an analytical expression:

$$\tau^{1/2} = \tau_0^{1/2} - (kT/2\alpha_0)\ln(\dot{\gamma}_0/\dot{\gamma}) \tag{5}$$

or

$$\tau^{1/2} = C + D\ln\dot{\gamma}, \tag{6}$$

where C and D are positive constants such that

$$C = \tau_0^{1/2} - D\ln\dot{\gamma}_0 \tag{7}$$

and

$$D = (kT/2\alpha_0) \tag{8}$$

Equation 6 shows that $\tau^{1/2}$ increases linearly with the increase in $\ln\dot{\gamma}$ such that the slope $[\mathrm{d}\tau^{1/2}/\mathrm{d}(\ln\dot{\gamma})]$ of the

$\tau^{1/2} - \ln\dot{\gamma}$ line fitted to the data at a given temperature T is equal to D. Since D is directly proportional to T (Eq. 8), the slope $[\mathrm{d}\tau^{1/2}/\mathrm{d}(\ln\dot{\gamma})] = D$ (Eq. 6) decreases linearly as T is lowered such that $D = 0$ at $T \to 0$ K. So, the value of the constant $C(= \tau_0^{1/2} - D\ln\dot{\gamma}_0))$ should decrease linearly with the rise in temperature T at which deformation is carried out.

The slip system responsible for the flow stress in the crystals with high intrinsic lattice friction can be identified on evaluating (i) the parameter n related to the critical maximum height, nb, of the kink-pair for saddle-point configuration, (ii) the Peierls energy per interatomic spacing along the screw dislocation U, (iii) the initial length L_0 of the screw-dislocation segment taking part in the unit activation process of yielding at $T \to 0$ K under the action of applied shear stress τ_0, and (iv) the activation volume, v_0 associated with τ_0. This can be achieved on using the model expressions [12]:

$$n^3 = \left(W_0/Gb^3\right)^2(4G/\tau_0) \tag{9}$$

$$U = (W_0/n)^2\left(1/Gb^3\right) \tag{10}$$

$$L_0 = b(4Gn/\tau_0)^{1/2} \tag{11}$$

$$v_0 = (1/4)nL_0b^2. \tag{12}$$

Analysis of experimental data

Strain-rate dependence of the CRSS

The dependence of 0.2% proof stress $\sigma_{0.2}$ on the tensile strain-rate $\dot{\varepsilon}$ has been illustrated in semi-logarithmic coordinates in Fig. 2. The triangles (▲) and squares (■) denote the values of $\sigma_{0.2}$ for W and Mo polycrystals, respectively, deformed at $\dot{\varepsilon}$ in the range 2.1×10^{-4}–4.2×10^{-3} s^{-1}. Each point denotes an average value of four independent measurements and error bars show the range of measured $\sigma_{0.2}$ values. The straight lines drawn through the data points by least-squares fit are encompassed by the relations:

$$\mathrm{W}\ (\blacktriangle) : \sigma_{0.2} = 842 + 36.0\ln\dot{\varepsilon} \tag{13}$$

$$\mathrm{Mo}\ (\blacksquare) : \sigma_{0.2} = 972 + 65.7\ \ln\dot{\varepsilon} \tag{14}$$

with the linear correlation coefficient $r = 0.994$ and 0.998, respectively. The values of r close to 1 indicate an excellent linear relationship between $\sigma_{0.2}$ and $\ln\dot{\varepsilon}$ for both the metals.

In order to analyze the data within the framework of the KPN model, we shall first obtain shear values of the 0.2% proof stress ($\tau_{0.2}$) and the strain rate ($\dot{\gamma}$) from the tensile ones ($\sigma_{0.2}$ and $\dot{\varepsilon}$) by using a Taylor factor 1/3, i.e., $\tau_{0.2} = \sigma_{0.2}/3$ and $\dot{\gamma} = 3\dot{\varepsilon}$. Furthermore, the shear value of 0.2% proof stress ($\tau_{0.2}$) will be taken as the CRSS (τ), and subscript 0.2 will be dropped hereafter. Thus the triangles (▲) and squares (■) in Fig. 3 denote the values of the square-root of CRSS ($\tau^{1/2}$) of W and Mo polycrystals, respectively, as a function of the shear strain-rate $\dot{\gamma}$ in semi-logarithmic coordinates. The straight lines drawn through the data points by least-squares fit are represented by the mathematical expressions:

$$\mathrm{W}\ (\blacktriangle) : \tau^{1/2} = 16.54 + 0.428\ \ln\dot{\gamma} \tag{15}$$

$$\mathrm{Mo}\ (\blacksquare) : \tau^{1/2} = 18.0 + 0.843\ \ln\dot{\gamma} \tag{16}$$

with the linear correlation coefficient $r = 0.999$ and 0.993, respectively.

Comparison of Eqs. 6 and 15 shows that for W polycrystal, $C = 16.54\ \mathrm{MPa}^{1/2}$ and $D = 0.428\ \mathrm{MPa}^{1/2}$. On

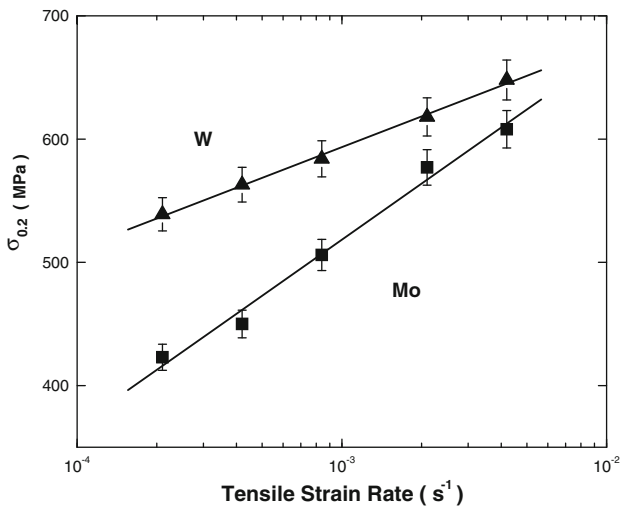

Fig. 2 The 0.2% proof stress ($\sigma_{0.2}$) of W and Mo polycrystals as a function of tensile strain-rate ($\dot{\varepsilon}$) in semi-logarithmic coordinates

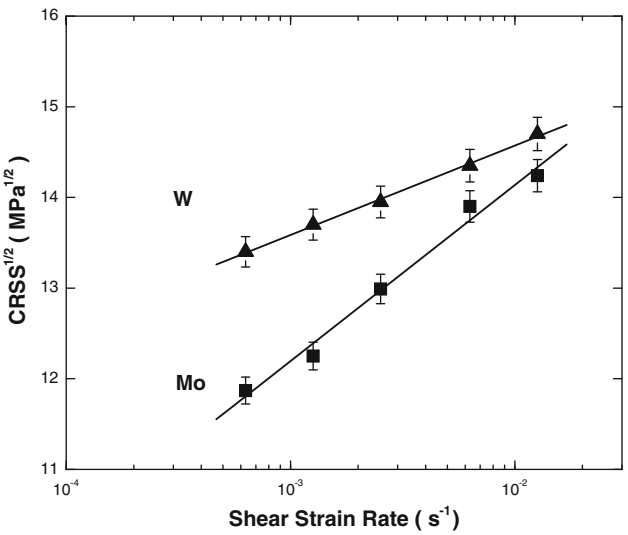

Fig. 3 The square-root of CRSS ($\tau^{1/2}$) of W and Mo polycrystals as a function of shear strain-rate ($\dot{\gamma}$) in semi-logarithmic coordinates

Table 2 Numerical values of the activation parameters of slip in W and Mo polycrystals via strain-rate dependence of the CRSS at room temperature

Metal	G (10^4 MPa)	b (nm)	Gb^3 (eV)	τ_0 (MPa)	α_0 (10^{-2} eV MPa$^{-1/2}$)	W_0 (eV)	W_{kp} (eV)	n	U (meV)	L_0 (b)	v_0 (b^3)	ln $\dot{\gamma}_0$	$\dot{\gamma}_0$ (s^{-1})	$\dot{\varepsilon}_0$ (s^{-1})
W (▲)	16.0	0.2741	20.6	617	3.00	0.742	1.484	1.10	21.7	33.9	9.4	19.11	1.99×10^8	6.64×10^7
Mo (■)	12.8	0.2725	16.7	1164	1.52	0.520	1.040	0.75	28.8	18.2	3.4	19.10	1.97×10^8	6.58×10^7

substituting the value of D in Eq. 8, one gets $\alpha_0 = 3.0 \times 10^{-2}$ eV MPa$^{-1/2}$. On taking $\tau^{1/2} = 14.02$ MPa$^{1/2}$, i.e., the average of five measured values of the square-root of CRSS denoted by triangles (▲) in Fig. 3, and putting it along with $m = \ln(\dot{\gamma}_o/\dot{\gamma}) = 25$, $T = 298$ K and $\alpha_0 = 3.0 \times 10^{-2}$ eV MPa$^{-1/2}$ in Eq. 5, one gets $\tau_0^{1/2} = 24.7$ MPa$^{1/2}$ or $\tau_0 = 617$ MPa. On using the expression $W_0 = \alpha_0 \tau_0^{1/2}$, one finds $W_0 = 0.742$ eV or $W_{kp} = 1.484$ eV. Also, on putting the values of C, D, and $\tau_0^{1/2}$ referred to above in Eq.7, the value of $\ln\dot{\gamma}_0$ is found to be 19.11, and hence $\dot{\gamma}_0 = 1.99 \times 10^8 s^{-1}$ or $\dot{\varepsilon}_0 = 6.64 \times 10^7 s^{-1}$, which is of the right order of magnitude, as envisaged in the KPN model.

Now, on using the appropriate values of G, Gb^3, τ_0, and W_0 (Table 2), various microscopic parameters of slip, i.e., n, U, L_0 and v_0, in W polycrystal can be readily obtained from Eqs. 9–12, and are given in Table 2. The value of the screw dislocation length $L_0 = 33.9b$ and that of the activation volume $v_0 = 9.4b^3$ involved in the unit activation process of yielding at $T \to 0$ K, are in good agreement with those specific to the Peierls mechanism, i.e., $L_0 = 20 - 50b$ [16, 17] and $v_0 = 1 - 100b^3$ [18–20]. The value of $n = 1.10$ being slightly greater than $[a_{(110)}/b] = 0.9428$ (Fig. 2) and substantially less than $[a_{(211)}/b] = 1.6329$ (Fig. 3) indicates that slip occurs preferentially on {110} planes. This is in accord with the observations of Kaun et al. [6] during the optical and electron microscopy of the slip lines on the surface of cylinder-shape specimens of W single crystals deformed at room temperature. This is further substantiated on comparing the kink-pair formation energy $W_{kp} = 1.48$ eV (Table 2) with that (1.3 eV) found by Brunner [21] for the formation of a pair of kinks on the $(a_0/2)\langle 111\rangle$ screw dislocation in {110} planes in W single crystal.

Similarly, analysis of $\tau^{1/2} - \ln\dot{\gamma}$ data pertaining to Mo polycrystals (Fig. 3) provides the values of model parameters $\alpha_0, \tau_0, W_0, W_{kp}, n, U, L_0, v_0, \dot{\gamma}_0$, and $\dot{\varepsilon}_0$ (Table 2). Here, the value of the screw dislocation length $L_0 = 18.2b$ and that of the activation volume $v_0 = 3.4b^3$ involved in the unit activation process of yielding at $T \to 0$ K, are in good agreement with those specific to the Peierls mechanism, whereas the kink-pair formation energy $W_{kp} = 1.08$ eV is in excellent agreement with that (1.08 eV) found by Suzuki et al. [22] for the nucleation of two individual kinks on a $(a_0/2)\langle 111\rangle$ screw dislocation in {110} planes in Mo single crystal. Moreover, the value of $n = 0.75$ being close to $[a_{(110)}/b] = 0.9428$ also points to $\{110\}\langle 111\rangle$ slip system being responsible for yielding of Mo polycrystal at room temperature. This is in excellent agreement with the slip line observations made on Mo single crystal deformed at room temperature by Kaun et al. [6].

Temperature dependence of the CRSS

Now we shall first examine the validity of the functional form of Eq. 4 in the case of temperature dependence of the CRSS of Mo, Nb, Fe, V, and K crystals, and then evaluate the microscopic parameters n, U, L_0, and v_0 of the KPN model of flow stress to ascertain the rate-controlling process of yielding in each case.

CRSS$^{1/2}$–T relationship

Reference to Fig. 4 shows the relationship between $\tau^{1/2}$ and T for the single crystals of Mo with $\langle 110\rangle$ orientation (impurities in wt ppm: C ≈ 2 to 3, N < 10, O < 1, and

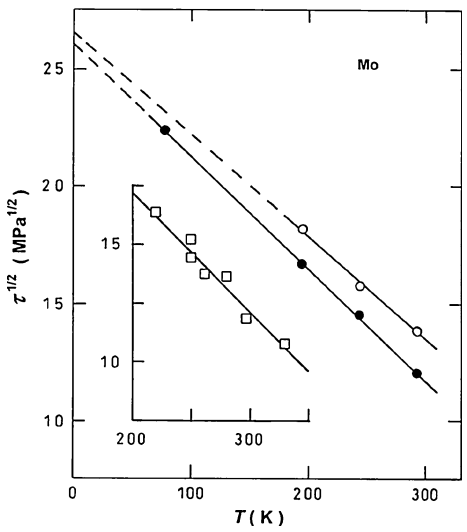

Fig. 4 Relation between $\tau^{1/2}$ and T for Mo single crystals (*open circle*, *filled circle*) and Mo polycrystals (*open square*). Data points were taken from Guiu and Pratt [7] and Malygin [14], respectively

Table 3 Numerical values of the positive constants A and B in Eq. 4 obtained by least-squares fit method from the $\tau^{1/2}$–T data for some bcc metals as well as those of some macroscopic parameters of the KPN model of flow stress

Metal	A (MPa)$^{1/2}$	B (10^{-2} MPa$^{1/2}$ K^{-1})	r	τ_0 (MPa)	α_0		W_0		T range (K)
					(10^{-24} N$^{1/2}$ m^2)	(10^{-2} eV MPa$^{-1/2}$)	(10^{-19} J)	(eV)	
Mo									
(○)	26.61	4.37	−0.998	708	3.95	2.46	1.051	0.656	195–293
(•)	26.09	4.77	−0.999	681	3.62	2.26	0.944	0.589	77–293
Mo (p) (□)	27.46	5.13	−0.979	754	3.36	2.10	0.922	0.576	220–330
Nb (•)	25.04	8.58	−0.994	627	2.02	1.26	0.506	0.316	77–195
	15.41	3.43	−0.999	237	5.02	3.14	0.774	0.484	195–295
Nb (○)	28.64	9.73	−0.996	820	1.78	1.11	0.507	0.317	10–77
Fe (•)	18.47	6.25	−0.977	341	2.75	1.72	0.509	0.318	77–125
	15.00	3.42	−0.998	225	5.04	3.15	0.757	0.473	125–298
Fe (○)	17.32	4.47	−0.993	300	3.86	2.41	0.668	0.417	125–298
V (p) (□)	20.04	6.00	−0.999	402	2.88	1.79	0.577	0.360	77–195
V (■)	17.9	5.74	−0.999	320	3.01	1.88	0.538	0.336	124–195
	13.3	3.45	−0.996	177	4.99	3.12	0.666	0.416	195–293
K (•)	1.55	3.06	−0.985	2.40	0.055	0.034	0.088	0.055	1.5–25

H < 0.01) deformed by Guiu and Pratt [7] at two different tensile strain-rates of 4.5×10^{-3} s^{-1}(○) and 4.5×10^{-5} s^{-1}(•) in the temperature range 77–293 K. In each case, the lines drawn through the data points by least-squares fit method comply with Eq. 4 with the values of constants A, B, and correlation factor r given in Table 3. Similarly, the empty squares (□) denote the $\tau^{1/2}$ values for 99.98% Mo polycrystal, 1 mm in diameter, and 20 mm in gauge length, stretched by Malygin [14] at a tensile strain-rate $\dot{\varepsilon} \sim 10^{-4}$ s^{-1} in the temperature interval 220–330 K. The shear values τ were obtained from the tensile flow stress $\sigma_{0.2}$ by using the Taylor factor 1/3 for a polycrystal, i.e., $\sigma = 3\tau$. The data points (□) are encompassed by Eq. 4 with the values of A, B, and r given in Table 3.

However, in the case of 99.8+ wt% Nb single crystals (impurities in wt%: H < 0.0005; C < 0.005; each Fe and Si < 0.01; N < 0.015; each Ni, Ti, Mo, W, Zr, and V < 0.02; O < 0.03; Ta < 0.05) deformed by Peter and Hendrickson [23] at a strain rate of 1.3×10^{-4} s^{-1}, the $\tau^{1/2}$ values depicted by filled circles (•) as a function of temperature T in Fig. 5 exhibit two distinct regimes in the $\tau^{1/2}$–T relationship. These are termed as low-temperature regime III and intermediate-temperature regime II—the nomenclature used by Brunner and Diehl [24], Brunner et al. [25], and Diehl et al. [26]. The high-temperature regime I in the CRSS–T curves of bcc refractory metals involves diffusional processes, and is therefore outside the scope of the KPN model [12] of flow stress. The straight lines fitted to the data points (•) by least-square fit method in both regime III (77–195 K) and regime II (195–295 K) are in accord with Eq. 4; the values of constants A, B, and correlation factor r in each case are given in Table 3. Moreover, the

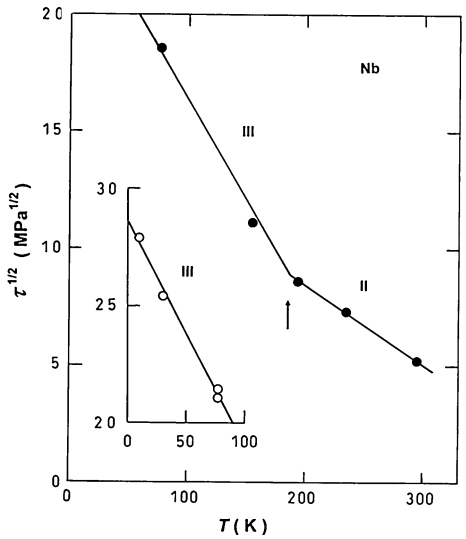

Fig. 5 Relation between $\tau^{1/2}$ and T for Nb single crystals. The data points (*open circle*) and (*filled circle*) were taken from Nagakawa and Meshii [9] and Peter and Hendrickson [23], respectively

open circles (○) in Fig. 5 denote the $\tau^{1/2}$ values [9] pertaining to zone-refined Nb single crystal ($\chi = 30°$, $\lambda = 45°$, Schmid factor = 0.612) with main metallic impurity 130 at. ppm and residual resistivity ratio about 2500. Before deformation, the specimens were purified by ultra-high vacuum annealing, and then deformed at a tensile strain-rate 4.6×10^{-4} s^{-1} at low temperatures in the range 10–77 K. A linear least-square fit to the data points (○) is achieved by means of Eq. 4 with the values of A, B, and r given in Table 3.

Likewise, Fig. 6 shows the relationship between $\tau^{1/2}$ and T for (•) zone refined single crystals of 99.999 wt% Fe

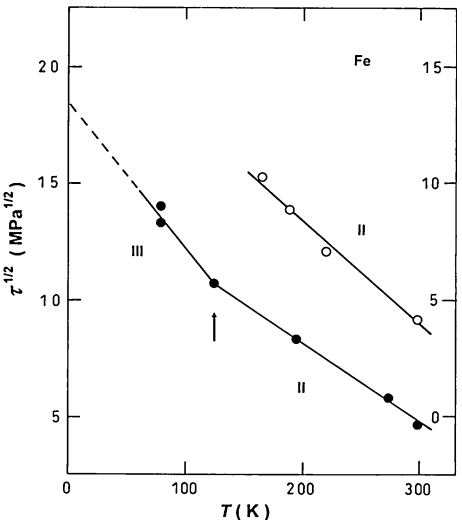

Fig. 6 Relation between $\tau^{1/2}$ and T for Fe single crystal. Data points (*open circle*) and (*filled circle*) were taken from Takeuchi et al. [28] and Horn et al. [27], respectively

(impurities in wt%: C $\approx$ 0.0008 and N $\approx$ 0.0003), and for (○) 99.982 wt% Fe single crystals (impurities in wt%: Mn $\approx$ 0.01, Si $\approx$ 0.001, P $\approx$ 0.001, C $\approx$ 0.002 and S $\approx$ 0.004) deformed by Horn et al. [27] and by Takeuchi et al. [28] at a strain rate of 1.7×10^{-4} s^{-1}, respectively. The lines drawn through the data points (•) and (○) by least-squares fit method in regime II (125–300 K) and regime III (78–125 K) are encompassed by Eq. 4 with the values of positive constants A and B, along with the correlation factor r, given in Table 3.

Referring to Fig. 7, the filled squares (■) denote the $\tau^{1/2}$ values of 99.99 wt% V single crystals (interstitial impurities $\approx$ 100 ppm in wt) deformed by Wang and Bainbridge [29] at a tensile strain rate $\dot{\varepsilon} = 6.7 \times 10^{-5}$ s^{-1} in the temperature range 124–293 K. Similarly, the empty squares (□) represent the $\tau^{1/2}$ values of 99.97 wt% V polycrystals (impurities in wt%: C $\approx$ 0.017, O $\approx$ 0.0042, N $<$ 0.001, H $\approx$ 0.007, Si $\approx$ 0.004, Zr $\approx$ 0.003) of 0.1 mm grain size, deformed by Yoshinaga et al. [30] at a tensile strain rate $\dot{\varepsilon} = 3.3 \times 10^{-5}$ s^{-1} in the temperature range 77–200 K. A Taylor factor of 1/3 was used to get the values of the CRSS τ from the tensile yield stress σ. The lines fitted to the data points (■) and (□) by least-squares fit method in regimes II and III, are encompassed by Eq. 4; the values of positive constants A and B, along with correlation factor r, are tabulated in Table 3.

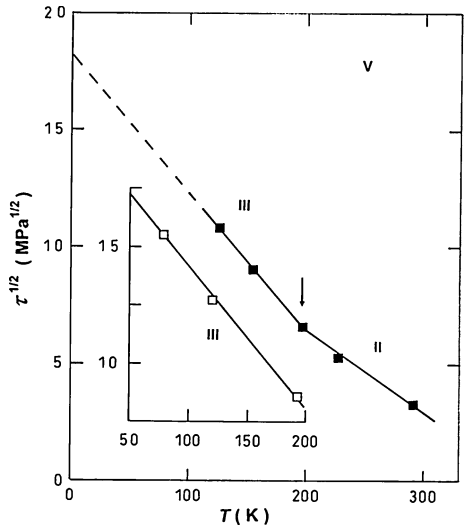

Fig. 7 Relation between $\tau^{1/2}$ and T for V single crystals (*filled square*) and V polycrystals (*open square*). The data points were taken from Wang and Bainbridge [29] and Yoshinaga et al. [30], respectively

Finally, Fig. 8 shows the relationship between the square-root of the CRSS, $\tau^{1/2}$, and the deformation temperature T, for 99.99% K single crystal (residual resistance ratio $R_{293}/R_{4.2} \sim 200$) with an orientation of $\chi = 0°$, $\psi = 55°$, i.e., centrally situated in the standard stereographic triangle. The crystal was deformed by Basinski et al. [31] in tension at a strain rate of 3.4×10^{-4} s^{-1} in the temperature range 1.5–30 K. Below a critical temperature $T_0 = 25$ K ($\approx$0.07 T_m, $T_m = 336$ K) the CRSS was found quite sensitive to the temperature at which deformation was carried out, whereas for $T \geq 25$ K it was insensitive to the temperature variation. The data points in Fig. 8 represent the $\tau^{1/2}$ values derived from the CRSS data of Basinski et al. [31]. The straight line drawn through the data points by least-squares fit method is encompassed by Eq. 4, with the values of constants A, B, and correlation factor r given in Table 3. The value of r being close to 1 indicates a good linear relationship between $\tau^{1/2}$ and T.

Identification of the slip system

The numerical values of the positive constants A and B (Table 3) determined as above help to evaluate τ_0, α_0, and

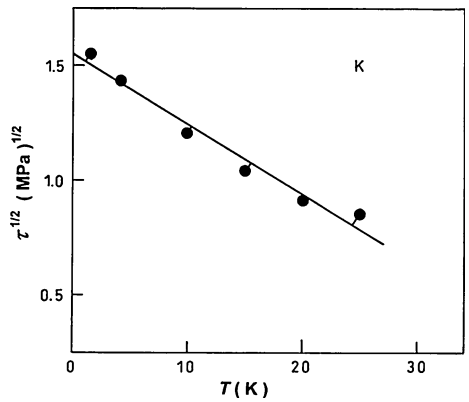

Fig. 8 Relation between $\tau^{1/2}$ and T for K single crystal. Data points were taken from Basinski et al. [31]

W_0 for Mo, Nb, Fe, V, and K crystals on using the mathematical expressions $A = \tau_0^{1/2}$, $B = mk/2\alpha_0$, and $W_0 = \alpha_0\tau_0^{1/2}$. Knowing the values of τ_0 and W_0 (Table 3), we shall now determine the magnitude of the microscopic activation-parameters n, U, L_0, and v_0 of slip with the help of Eqs. 9–12 derived in the KPN model of flow stress [12].

Using the appropriate values of G, Gb^3, τ_0 and W_0 for a given metal in Eq. 9, the parameter n related to the critical maximum height of the kink-pair for saddle-point configuration is evaluated. Putting this value together with those of W_0 and Gb^3 in Eq. 10, one obtains U, i.e., the Peierls energy per interatomic spacing along the screw dislocation. Substitution of G, τ_0, and n values in Eq. 11 yields L_0, while Eq. 12 helps to evaluate the activation volume v_0 on making use of n and L_0 values (Table 4). It can be readily seen that the values of L_0 and v_0 for Mo, Nb, Fe, V, and K listed in Table 4 are in good agreement with those specific to Peierls mechanism, i.e., $L_0 = 20 - 50b$ [16, 17] and $v_0 = 1 - 100b^3$ [18–20]. Also, the kink-pair formation energy W_{kp} (Table 4) is of the right order of magnitude in each case.

To identify the slip system operative in these metals, we shall now base our considerations on the n values given in Table 4. In the case of molybdenum, the critical maximum height nb of the kink-pair for saddle-point configuration is found to be $0.95b$ for Mo polycrystal, and $1.06b$ for Mo single crystals for deformation temperature between 77 and 330 K. These values are in good agreement with the Peierls valley separation $a_{(110)} = 0.9428b$, which indicates that slip occurs on {110} planes of Mo crystals in the temperature range referred to above. Also, the kink-pair formation energy $W_{kp} = 1.15$–1.35 eV (Table 4) is in good agreement with the values 1.08–1.40 eV reported in the literature [22, 32, 33] for the nucleation of two individual kinks on a $(a_0/2)\langle 111\rangle$ screw dislocation in {110} planes in Mo single crystals. It is worthy of note that the slip system $\{110\}\langle 111\rangle$ operative in Mo polycrystal at room temperature determined via strain-rate dependence of CRSS in this experimentation is in good agreement with that determined above via temperature dependence of the CRSS at a given strain-rate. This is also supported by the slip-line observations of Guiu and Pratt [7] made on Mo single crystals that at rather low temperatures slip occurred predominantly on {110} planes while some traces of slip were also found on {211} planes. However, at temperatures ≥353 K slip occurred on {211} planes only.

As far as niobium is concerned, the values of $n = 0.85$ and 0.93 in regime III (10–195 K) and $n = 1.71$ in regime II (195–295 K) are in excellent agreement with $[a_{(110)}/b] = 0.9428$ and $[a_{(211)}/b] = 1.6329$, respectively. This shows that slip systems for yielding of Nb single crystal in the low- and intermediate-temperature domains are $\{110\}\langle 111\rangle$ and $\{211\}\langle 111\rangle$, respectively. Nagakawa and Meshii [9] have also inferred from their slip-line observations made on Nb single crystals deformed at 4.2–77 K that flow stress is controlled by the glide of $(a_0/2)\langle 111\rangle$ screw dislocations on {110} planes at such low temperatures. The value of kink-pair formation $W_{kp} = 0.63$ eV (Table 4) in regime III is also in good agreement with the enthalpy of formation (0.65 ± 0.02 eV) of a pair of isolated kinks on $(a_0/2)\langle 111\rangle$ screw dislocations in {110} planes in Nb single crystals [34].

For iron single crystals, the n values being equal to 1.46 and 1.75 for intermediate temperatures (125–298 K) in regime II, indicate that the critical maximum height nb of the kink-pair for saddle-point configuration is quite close to the Peierls valley separation $a_{(211)} = 1.6329b$, which means that slip occurs on {211} planes. This is in accord

Table 4 Numerical values of the activation-parameters of slip in some bcc metals

Metal	G (10^4 MPa)	b (nm)	Gb^3 (eV)	W_{kp} (eV)	n	U (meV)	L_0 (b)	v_0 (b^3)	T range (K)
Mo									
(○)	12.8	0.2725	16.1	1.312	1.06	23.7	27.7	7.3	195–293
(•)				1.178	1.00	21.5	27.4	6.9	77–293
Mo (p) (□)				1.152	0.95	22.8	25.4	6.0	220–330
Nb (•)	3.7	0.2858	5.39	0.632	0.93	21.4	14.8	3.4	77–195
				0.968	1.71	14.9	32.7	14.0	195–295
Nb (○)				0.634	0.85	25.5	12.4	2.6	10–77
Fe (•)	8.1	0.2482	7.73	0.636	1.17	9.6	33.3	9.7	77–125
				0.946	1.75	9.5	50.2	22.0	125–298
Fe (○)				0.834	1.46	10.6	39.8	14.5	125–298
V (p) (□)	4.6	0.2622	5.18	0.720	1.30	14.8	24.4	7.9	77–195
V (■)				0.672	1.34	12.1	27.8	9.3	124–195
				0.832	1.88	9.5	44.2	20.8	195–293
K (•)	0.12	0.4544	0.70	0.109	2.31	0.81	68.0	39.3	1.5–25

with the slip-line observations of Spitzig and Keh [35], who reported a strong tendency to slip on {211} planes in α-Fe single crystals at such temperatures. Moreover, the value of nb found to be equal to $1.17b$ for low temperatures (77–125 K) in regime III is close to $a_{(110)} = 0.9428b$, which shows that slip occurs predominantly on {110}planes of α-Fe single crystals, confirmed by slip traces observed by Aono et al. [36] on deformed iron crystals at rather low temperatures. This is further supported by the fact that $W_{kp} = 0.64$ eV is in good agreement with that (0.60 eV) required for kink-pair formation in the $(a_0/2)\langle 111\rangle$ screw dislocations on {110} planes in α-Fe single crystals in low-temperature regime III [37].

In the case of vanadium, the n values 1.30 for V polycrystal and 1.34 for V single crystal in low-temperature regime III (77–195 K) are between $[a_{(110)}/b] = 0.9428$ and $[a_{(211)}/b] = 1.6329$, which indicates that slip occurs simultaneously on {110}and {211} planes. Moreover, $n = 1.88$ for V single crystal in intermediate-temperature regime II (195–293 K) is close to $[a_{(211)}/b] = 1.6329$ rather than $[a_{(321)}/b] = 2.4945$, meaning thereby that {211} slip plane is dominant in the intermediate-temperature regime II. Though Wang and Bainbridge [29] consider the interaction between dislocations and interstitial impurities as the dominant rate-controlling process of yielding between 200 and 293 K, yet the derived values $L_0 = 44.2b$ and $v_0 = 20.8b^3$ (Table 4) lend support to Peierls mechanism as the rate-controlling process of deformation.

Finally, one can ascertain the rate-controlling process of yielding in K single crystal ($T = 1.5$–25 K) on noting from Table 4 the values of n, L_0, and v_0 for this metal. The value of $n = 2.27$, which is close to $[a_{(321)}/b] = 2.4945$ (Fig. 9), points to slip on {321} plane, whereas the values of $L_0 = 67b$ and $v_0 = 38b^3$ are specific to Peierls mechanism

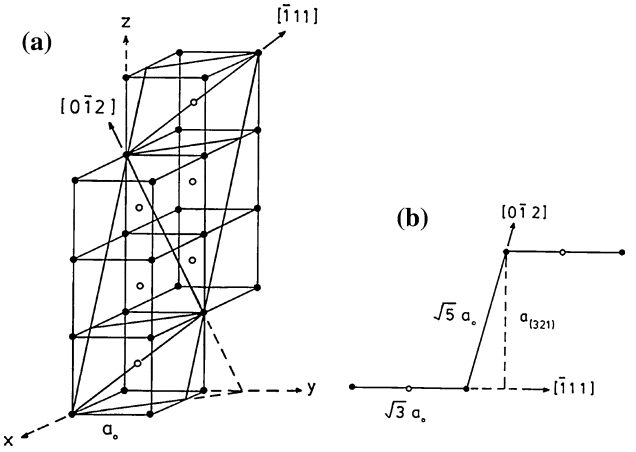

Fig. 9 Schematic representation of **a** the (321) $[\bar{1}11]$ slip system, and **b** the separation $a_{(321)} = \sqrt{5}a_0 \sin 75.04^\circ = 2.1603a_0 = 2.4945b$ between two neighboring Peierls valleys along $[\bar{1}11]$ direction in (321) plane

[16–20] as the rate-controlling process of yielding. The slip system operative in K single crystal in regime III is therefore $\{321\}\langle 111\rangle$.

Summary and conclusions

1. The analytical formulations of the KPN model of flow stress satisfactorily accounts for the observed temperature and strain-rate dependences of the CRSS of crystals with high intrinsic lattice friction. Evaluation of the microscopic parameters of slip helps to identify the deformation mechanism and active slip-systems responsible for yielding at temperatures where diffusional processes are dormant.
2. The strain-rate dependence of the CRSS of W and Mo polycrystals deformed at room temperature points to $\{110\}\langle 111\rangle$ as the preferentially active slip-system for deformation via Peierls mechanism, which is supported by the slip-line observations made on the surface of W and Mo single crystals reported in the literature.
3. The temperature dependence of the CRSS, τ, of bcc metals (Mo, Nb, Fe, V, and K) follows a linear relationship between $\tau^{1/2}$ and T both at low temperatures (regime III) as well as at intermediate temperatures (regime II).
4. The rate-controlling process of yielding in Mo crystals, whether mono or polycrystalline, in the temperature range 77–330 K is $\{110\}\langle 111\rangle$ type glide of screw dislocations.
5. The CRSS of Nb (10–195 K) and Fe (77–125 K) single crystals in the low-temperature regime III is determined by $\{110\}\langle 111\rangle$ slip system, whereas in the intermediate-temperature regime II the active slip-system in Nb (195–295 K) and Fe (125–298 K) is $\{211\}\langle 111\rangle$.
6. The CRSS of both V single and polycrystal in the low-temperature regime III (77–195 K) is determined by simultaneous slip on {110} and {211} planes. However, {211} slip-planes are preferentially active in V single crystals in the intermediate-temperature regime II (195–293 K).
7. Peierls mechanism is the rate-controlling process of yielding in K single crystals at rather low temperatures (1.5–25 K). The screw dislocations trapped in Peierls valleys along $\langle 111\rangle$ directions participate in the slip process on {321} planes.

References

1. Orowan E (1934) Z fuer Phys 89:605
2. Polanyi M (1934) Z Phys 89:660
3. Taylor G (1934) Proc R Soc A 145:363

4. Taylor G (1934) Proc Roy Soc A145:388
5. Zamiri AR, Pourboghrat F (2010) Int J Plast 26:731
6. Kaun L, Luft A, Richter J, Schulze D (1968) Phys Stat Sol 26:485
7. Guiu F, Pratt PL (1966) Phys Stat Sol 15:539
8. Takeuchi S, Maeda K (1977) Acta Metall 25:1485
9. Nagakawa J, Meshii M (1981) Phil Mag A 44:11651
10. Wasserbach W (1995) Phys Stat Sol (a) 147:417
11. Seeger A, Wasserbach W (2002) Phys Stat Sol (a) 189:27
12. Butt MZ (2007) Phil Mag 87:3595
13. Butt MZ, Khaleeq-ur-Rahman M, Dilawar Ali (2009) J Phys D Appl Phys 42:035405
14. Malygin GA (2005) Phys Solid State 47:896
15. Feltham P, Kauser N (1990) Phys Stat Sol (a) 117:135
16. Arsenault RJ (1967) Acta Metall 15:501
17. Feltham P (1969) J Phys D Appl Phys 2:377
18. Abed FH, Voyiadjis GZ (2005) Acta Mech 175:1
19. Little EA (1976) J Aust Inst Metals 21:50
20. Nemat-Nasser S, Guo W, Liu M (1999) Scripta Mater 40:859
21. Brunner D (2000) Mater Trans JIM 41:152
22. Suzuki T, Koizumi H, Kirchner HOK (1995) Acta Metall Mater 43:2177
23. Peters BC, Hendrickson AA (1970) Metall Trans 1:2271
24. Brunner D, Diehl J (1987) Phys Stat Sol (a) 104:145
25. Brunner D, Diehl J, Seeger A (1984) In: Paidar V, Lejcek L (eds) The structure and properties of crystal defects. Elsevier Publishing Co, Amsterdam, p 175
26. Diehl J, Schreiner M, Staiger S, Ziesele S (1976) Scripta Metall 10:949
27. Horne GT, Roy RB, Paxton HW (1963) J Iron Steel Inst 201:161
28. Takeuchi S, Yoshida H, Taoka T (1968) Trans Jpn Inst Met Suppl 9:715
29. Wang CT, Banbridge DW (1972) Metall Trans 3: 3161
30. Yoshinaga H, Toma K, Abe K, Morozumi S (1971) Phil Mag 23:1387
31. Basinski ZS, Duesbery MS, Murty GS (1981) Acta Metall 29:801
32. Conard H, Hayes W (1963) Trans ASM 56:249
33. Groger R (2007) Development of physically based plastic flow rules for body-centered cubic metals with temperature and strain rate dependencies. PhD Thesis, University of Pennsylvania
34. Ackermann F, Mughrabi H, Seeger A (1983) Acta Metall 31:1353
35. Spitzig WA, Keh AS (1970) Metall Trans 1:2751
36. Aono Y, Kuramoto E, Kitajima K (1981) Rep Res Inst Appl Mech 29:127
37. Brunner D, Diehl J (1991) Phy Stat Sol (a) 124:455